

ORIGINAL RESEARCH ARTICLE

Inventory of dykes and their tectonic environment in S-Algeria, N-Mali and N-Niger based on a GIS embedded comparative analysis of remote sensing data

Barbara Theilen-Willige

Faculty IV (retired), Technische Universität Berlin (TUB), 10623 Berlin, Germany. E-mail: barbara.theilen-willige@t-online.de

ABSTRACT

Although dykes are a predominant and widely distributed phenomenon in S-Algeria, N-Mali and N-Niger, a systematic, standardized inventory of dykes covering these areas has not been published so far. Remote sensing and geo information system (GIS) tools offer an opportunity for such an inventory. This inventory is not only of interest for the mining industry as many dykes are related to mineral occurrence of economic value, but also for hydrogeologic investigations (dykes can form barriers for groundwater flow). Surface-near dykes, major fault zones, volcanic and structural features were digitized based on Landsat 8 and 9, Sentinel 2, Sentinel 1 and ALOS PALSAR data. High resolution images of World Imagery files/ESRI and Bing Maps Aerial/Microsoft were included into the evaluations. More than 14,000 dykes were digitized and analyzed. The evaluations of satellite images allow a geomorphologic differentiation of types of dykes and the description of their characteristics such as dyke swarms or ring dykes. Dykes are tracing zones of weakness like faults and zones with higher geomechanically strain. Dyke density calculations were carried out in ArcGIS to support the detection of dyke concentrations as stress indicator. Thus, when occurring concentrated, they might indicate stressed areas where further magmatic and earthquake activity might potentially happen in future.

Keywords: Dykes; Remote Sensing; GIS; South-Algeria; North-Mali; North-Niger

ARTICLE INFO

Received: 8 May 2023
Accepted: 15 June 2023
Available online: 28 June 2023

COPYRIGHT

Copyright © 2023 by author(s).
Journal of Geography and Cartography is published by EnPress Publisher LLC. This work is licensed under the Creative Commons Attribution-NonCommercial 4.0 International License (CC BY-NC 4.0).
<https://creativecommons.org/licenses/by-nc/4.0/>

1. Introduction

Dyke swarms represent conspicuous extensional structures and are widespread in S-Algeria, N-Mali and N-Niger. Although especially mafic dykes are a predominant phenomenon in these countries, a systematic, standardized inventory of dykes covering these areas has not been published so far, although several regions have been investigated quite detailed^[1].

Remote sensing and GIS tools offer an opportunity for such an inventory^[1-3]. Such an inventory of dykes is not only of interest to the mining industry as many dykes are related to mineral occurrence of economic value, but also for hydrogeologic investigations. Dykes can act either as good conductors or as barriers to groundwater flow. Whether dykes act as water barriers or conductors, depend on factors such as their structures, their intensity of fracturing locations and orientations with respect to the groundwater flow^[4].

Another reason is the research for geohazards related to dykes. During a volcanic unrest period with dyke injection, one of the main scientific tasks is to assess the geometry and the propagation path of the dykes. In volcano-tectonic regions, dyke propagation from shallow magmatic chambers is often controlled by the interaction of the local and regional stress fields. The variations of the stress fields result from

a combination of factors such as the regional tectonic strain, the geometry of pressurized magma chambers, the layering and the pre-existing discontinuities^[4-7]. Thus, the detailed inventory of dykes visible at the surface can contribute to gain information of a paleo-stress field up to information of a more recent stress pattern. Most dykes are situated within extension fractures as indicated by the present field observation and supported by studies worldwide^[7]. However, when looking at the World Stress Map (2016), there are very few data of the investigation area available^[8]. Therefore, the systematic assessment and mapping of dykes can contribute to the knowledge about stress fields. Dykes are tracing zones of weakness and zones with higher geomechanically stress, at least at the time of their development. When occurring concentrated, they can indicate areas where further magmatic and earthquake activity or aseismic long-term movements might happen again, such as by

reactivation of fault zones. Little is known so far about the effect of stronger earthquakes on magmatic activity in the investigation areas. No documentations related to correlations of stronger earthquakes and volcanic eruptions could be found.

It was not investigated so far as well, how larger cosmic impacts (meteorites and asteroids) of different ages in the investigation area (**Figure 1**) might have had an influence on magmatic activity, especially on dyke development in the surrounding area of impact craters. It can be assumed that high velocity impact of asteroids and larger meteorites might initiate magmatic activity, whenever magma chambers under significant pressure within the magma storage region are existing in the target area. They may cause melting and deep deformations that eventually can lead to volcanic eruptions in those areas already susceptible to volcanic activity^[9].

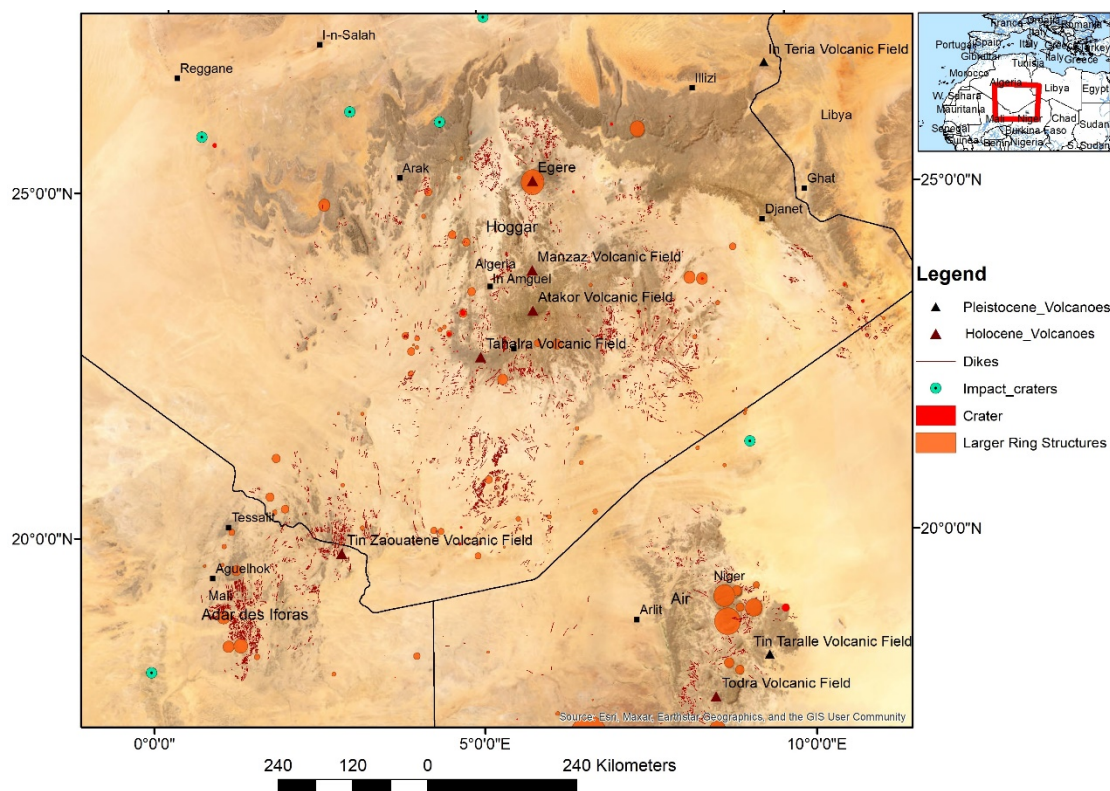


Figure 1. Overview of digitized dykes (more than 14,000) in the investigation area including impact crater data from the Planetary and Space Science Centre (PASSC), Canada^[11] and digitized ring structures and craters (crater used as neutral morphological term regardless the origin).

2. Geographic and geologic overview

The investigation area includes the Hoggar

mountains in S-Algeria with height levels up to 2,900 m, the Air mountains in N-Niger reaching height levels up to 2,000 m and the Adrar des Iforas in NE-Mali with height levels between 800–900 m

in an arid environment with hot desert climate (**Figures 1 and 2**). It meets all criteria for a geodynamic active landscape like linear step-like fault-scarps, traces of volcanic activity (as scoria cones, lava fields, maars), and numerous dykes. Most of the visible dykes are situated is height levels above 500 m. If there are dykes in lower regions, it must be assumed that they are covered by younger sediments and, thus, cannot be detected on the satellite

images and in the field. The visible dyke occurrence is clearly related to the mountainous areas. Contrasting morphologies, which result from recent tectonic uplift, erosion of the basement, and different volcanic eruptive styles, dominate the landscape. Outpouring of mafic magmas produced extensive lava flows that form large, dissected plateaus, or have filled valleys associated with scoria cones and necks^[10].

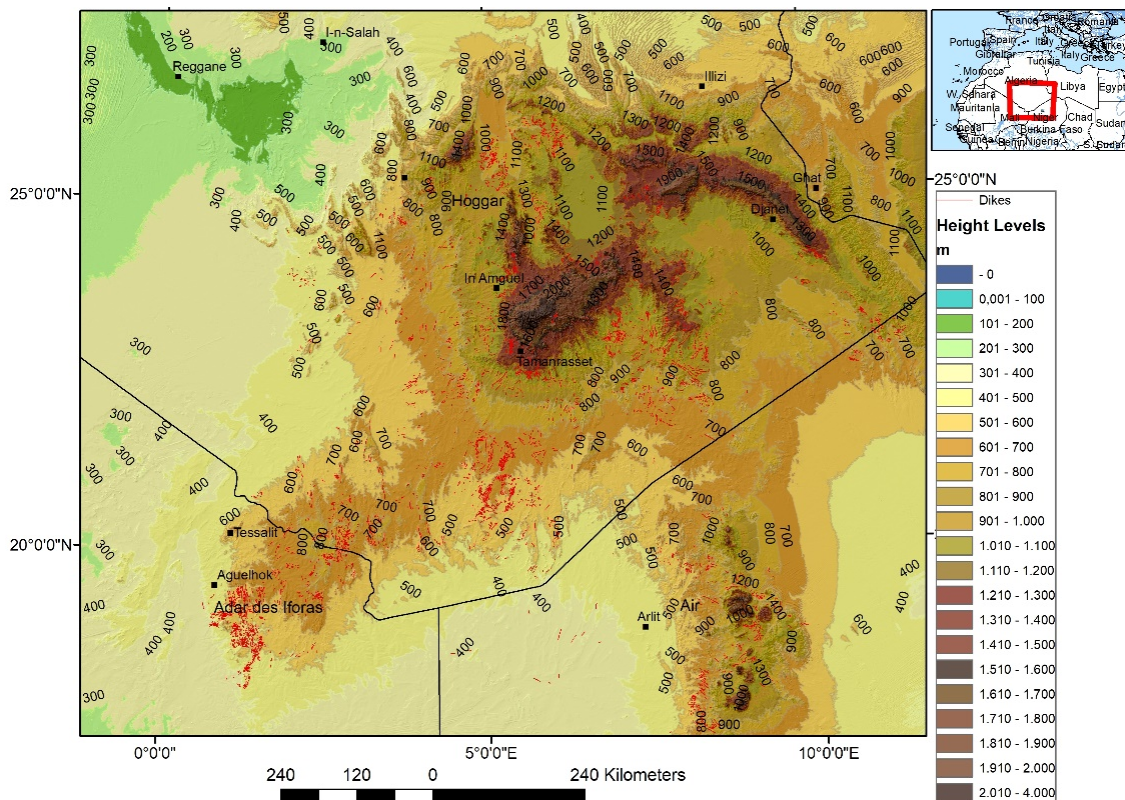


Figure 2. Height level map based on GEBCO height data^[12].

The Hoggar Massif in South-Algeria is associated with the exposed Pan-African basement extending over an area greater than 550,000 km²^[13,14]. The Hoggar mountains form the main part of the Tuareg Shield, which contains Archaean/Palaeoproterozoic and Neoproterozoic terranes, unconformably overlain by subhorizontal Palaeozoic sediments. The Tuareg Shield is an assemblage of about 25 terranes separated by mega-shear zones developed during the convergence between the West African craton to the west and the Saharan metacraton to the east at the end of the Neoproterozoic (630–580 Ma), which corresponds to the Pan-African orogeny^[14]. The Tuareg Shield developed during the late Neoproterozoic Pan-African orogeny (**Figure 3**). The major structural domains

of the Tuareg Shield are the “Polycyclic Central Hoggar” to the east and the “Western Hoggar”, or “Pharusian Belt”, to the west^[15]. A long-wavelength regional uplift, centered on the Hoggar Massif, occurred during the Cenozoic extending over a distance of more than 1,500 km from north to south was confirmed by Ouzegane *et al.*^[14].

The volcanism in the investigation area is linked to the mantle structure down to 150 km, implying a shallow mantle source^[18]. In response to stress resulting from the Africa-Europe collision, volcanism may be generated by adiabatic pressure release of an uprising asthenosphere. The reactivation of preexisting, ductile shear zones and fractures generated during the Pan-African (late Neoproterozoic) orogeny played an important role.

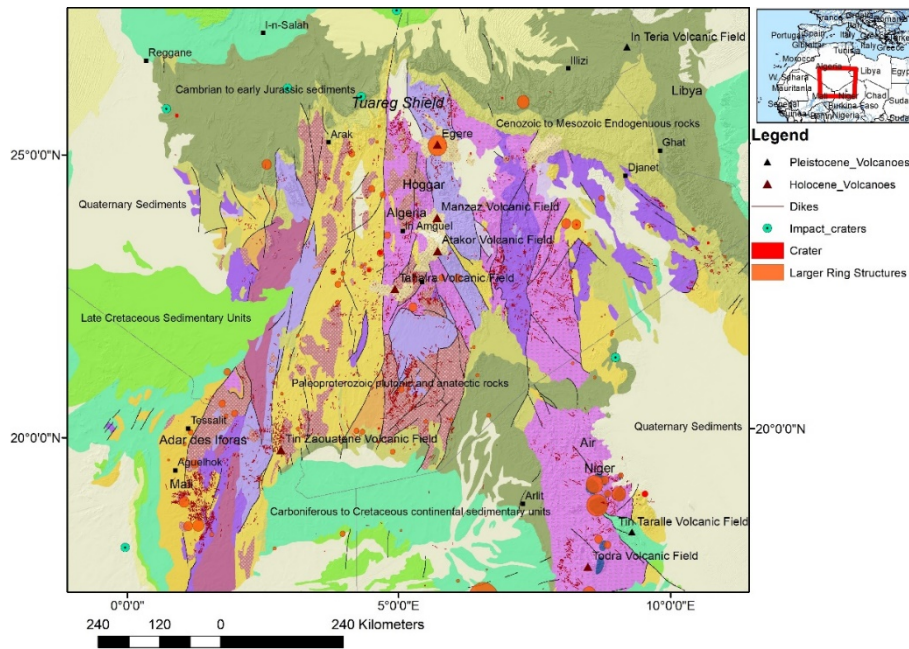


Figure 3. Geologic overview (downloaded from the OneGeology Portal^[16] including impact crater data from the Planetary and Space Science Centre (PASSC), Canada^[17] and digitized ring structures and craters.

Subsequent vertical movements along the north-south subvertical shear zones of the Tuareg Shield, resulting into slight deformations, angular unconformities and variations in the Tassilis sandstone thickness, are recorded in the sedimentary sequences^[10]. Deformation is strongly influenced by structural position and mechanical properties of the rocks during the deformation.

There are several volcanic districts located in Hoggar, Massif, N-Mali and N-Niger^[19–22]. The volcanic events produced composite flood lavas (plateau basalt) essentially made of alkali olivine basalts. Trachytic and phonolitic plugs are associated with these phases^[18,19].

3. Materials and methods

This study aims to contribute to the inventory of different types of dykes, their occurrence and morphologic characteristics based on a comparative analysis of different satellite data: Landsat 8 and 9, Sentinel 2, Sentinel 1 and the Advanced Land Observing Satellite-1 (ALOS), Phased Array type L-band Synthetic Aperture Radar (PALSAR) data from the Japan Aerospace Exploration Agency (JAXA). The evaluations were combined with digital elevation model (DEM) data (**Figure 4**). Large areas in the arid environment of the investigation

area are covered by aeolian sediments. Radar images with their ability to penetrate these dry, loose sedimentary covers (about more than 1 m) support the identification even of buried dykes due to their stronger radar reflection.

The interdisciplinary approach used in the scope of this research includes evaluations of remote sensing data, geological, and topographic data, integrated into a GIS environment. Satellite imageries and Digital Elevation Model (DEM) data were used then for generating a dyke related GIS data base. DEM data such as General Bathymetric Chart of the Oceans (GEBCO, spatial resolution of 450 m) data, or from the Shuttle Radar Topography Mission (SRTM) and ASTER DEM (both 30 m spatial resolution), are covering the whole investigation area. The Advanced Land Observing Satellite-1 (ALOS), Phased Array type L-band Synthetic Aperture Radar (PALSAR) provided data with 12.5 m spatial resolution, however, not as a complete coverage. The satellite data were downloaded from open sources such as the USGS/Earth Explorer^[23], the Sentinel Hub/ESA^[24], and the Alaska Satellite Facility (ASF)^[25].

The satellite data were processed and evaluated such as Sentinel 1 C-Band, Synthetic Aperture Radar (SAR) and ALOS PALSAR L-Band data

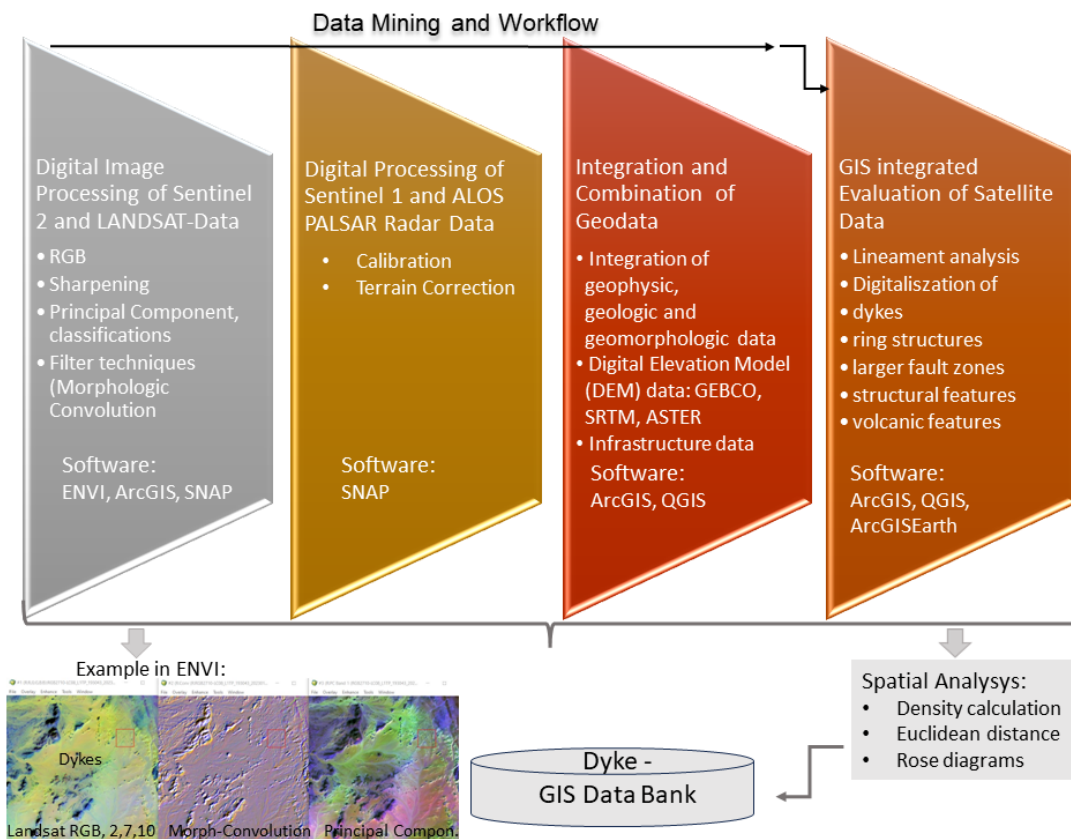


Figure 4. Creating a dyke data bank.

and optical Sentinel 2 images, and Landsat optical data (Landsat TM and Landsat 8 and 9 of the Operational Land Imager-OLI) using digital image processing software as the Sentinel Application Platform (SNAP)/ESA and ENVI/L3Harris Geospatial Solutions as well as the geoinformation systems ArcGIS/ESRI and QGIS. Digital image processing of Landsat 8/9 data was carried out by merging different Red Green Blue (RGB) band combinations, especially the thermal bands. Thermal inertia controlling surface temperatures support the identification of dykes as their reflection in the thermal band is different from the environment.

The evaluation of the equal data sets such as Landsat RGB images combining the Bands 2, 7 and 10, enhanced with Band 8 (15 m spatial resolution), Sentinel 2 RGB images, combining the Bands 2, 8 and 4, with 10 m resolution, ALOS PALSAR L-Band images and Sentinel 1 radar data (11 m) from the large investigation area allows the mapping of dykes under nearly the same conditions. Of course, the acquisition times of the data are different causing varying surface reflectance conditions, for example due to sandstorms or to rare precipitations.

However, the uniform data processing and evaluation of the same data sets leads to a standardized inventory of dykes. High resolution images of World Imagery files/ESRI and Bing Maps Aerial/Microsoft, and ArcGIS Earth/ESRI were included into the evaluations.

Dykes, volcanic features (scoria cones, craters), major lineaments and structural units (synclines, anticlines, ring structures) were digitized visually based on the comparative analysis of the different satellite data.

4. Inventory of dykes

Satellite images provide an overview of the various types of dykes in the arid investigation areas with few larger cities and settlements. Their detectability depends on their mineralogic composition, their age, grade of weathering and erosion, and their tectonic environment. The age of dykes varies significantly as they belong to several “generations” in the earth’s history. Many dykes were prone to different degrees of mylonitization and recrystallization^[17]. The dyke trends, in general, are assumed to be perpendicular to the direction of the

minimum compressive principal stress at the time of the dyke emplacement. Some dykes are inclined, but the great majority are subvertical. Most of the dykes form parallel ridges with distinct edges, whereas other dykes are more irregular in shape. Many dykes in the research area are either underlapping or overlapping. Where dyke segments overlap, they normally become thinner. Dykes are often more resistant to weathering and erosion than their host rocks. The contacts between dykes and their host rocks are generally distinct.

Of course, only the surface-near dykes can be detected on remote sensing data, as dykes situated underneath the surface more than several meters are difficult or not possible to trace with remote sensing methods, not even with long-wave L-Band

radar data. Nevertheless, more than 14,000 dykes could be digitized.

The following main geomorphologic types can be distinguished (**Figure 5**).

- a. Long, linear and narrow dykes (width: about 20–40 m) extended over vast distances with more than several kilometers with nearly no interruptions.
- b. Shorter dykes occurring in dense, most linear or curvi-linear, parallel swarms.
- c. Shorter dykes interrupted by small scoria cones and plugs of varying sizes.
- d. Shorter dykes with a varying width of intrusions.
- e. Ring dykes surrounding larger magmatic bodies.

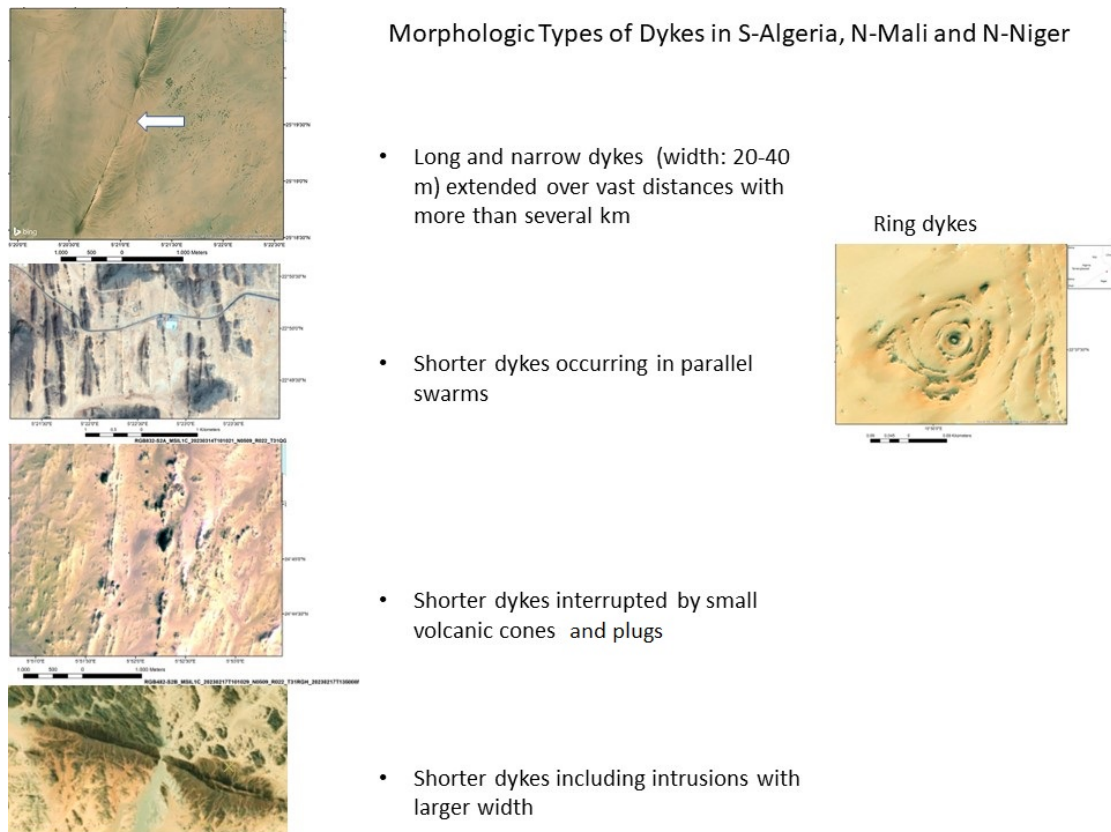


Figure 5. Examples of the main geomorphologic types of dykes.

The dyke type (d) seems to be the youngest type as those dykes are intersecting and overlapping previous ones and they show hardly any signs of weathering and erosion. Sometimes all these different types can be found together nearby in one area. However, dense dyke swarms occur concentrated in those areas, where obviously the strain

partitioning between structures at different structure levels allows dyke intrusion. The geomechanically conditions of the particular rock units and structural setting seem to determine more the dyke intrusions, rather than as the outcome of consecutive deformation phases related to different far-field stresses. As variations in tectonic stress re-

gimes and magma-supply rate, as well as the presence of pre-existing structural discontinuities can affect intrusion dynamics, dykes are very useful paleo-stress indicators.

Some of the factors influencing the development and shape of dykes comprise the regional and local stress conditions, fault and fracture zones and reactivation of existing faults, the occurrence of ring structures, anti- and synclines, previous magmatic and tectonic activity, vertical and horizontal movements, and earthquake activity. For example, the intrusion of dykes often follows ring faults surrounding plutons or volcanos, or the axis of anticlines.

The varying intensity and velocity of uplifting movements causing the “opening” of fracture zones has to be taken into account. However, there

are no precise geodetic data about vertical movements available so far.

As wind erosion often creates parallel linear abrasion patterns, mainly in SW-NE direction, within outcropping rocks, the identification of dykes becomes difficult in those areas. Longitudinal dunes and aeolian sheets can be forming a hindrance for the identification as well. Therefore, the specific local conditions have to be considered when analyzing dykes in the affected areas.

As information of dyke ages are still not available for large areas, relatively age differences can be derived from satellite images by detecting younger dykes cutting through older ones (**Figures 6 and 7**, 1—older, and 2—younger). By combining the information of the satellite image evaluations with geologic maps, it can be inferred often from the age of the hosting rocks the later dyke intrusion.

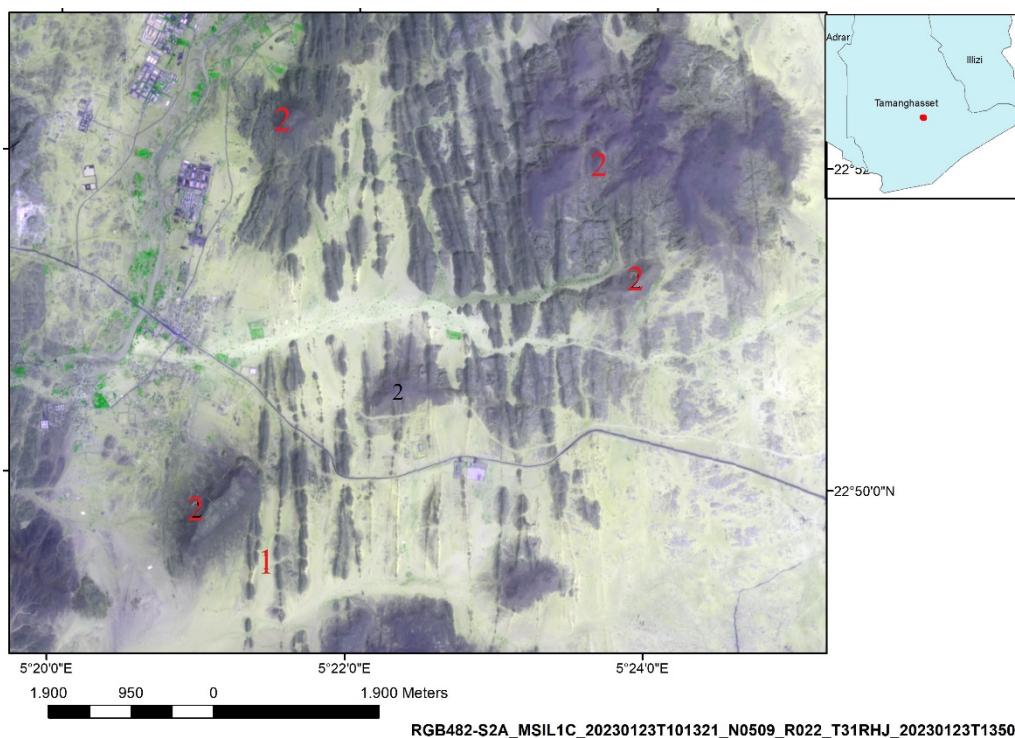


Figure 6. Overlapping dykes of different ages and composition in the Central-Hoggar mountains (1—older dykes, 2—younger dykes) visible on a Sentinel 2-scene.

In **Figure 7**, dykes are cutting through the lava sheets of the Egeré volcanic field in the central part of the Hoggar mountains and, thus, are younger than the lava.

When investigating whether there are typical structural settings for the occurrence of dyke swarms it appears that dykes can be observed within and along the large N-S striking, ductile

shear zones, especially in the area between larger shear zones, and concentrated between and around larger ring structures. Large plutons, now forming domes, obviously seem to be a hindrance for uprising dykes as there are only few plutons intersected by dykes. Within deeply eroded batholites forming concentric basins, however, ring dykes and dyke swarms can be observed.

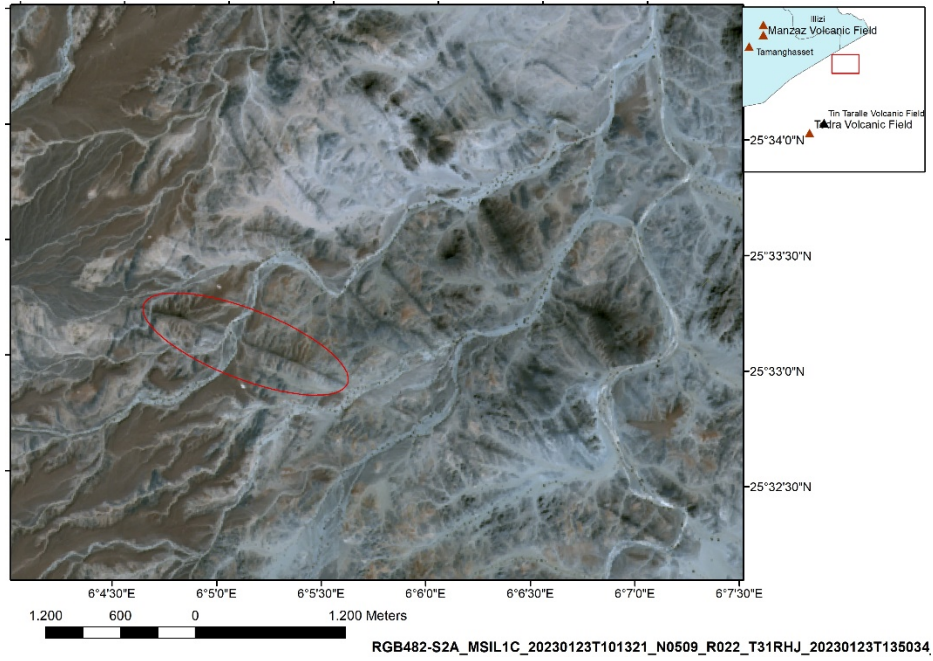


Figure 7. Dykes cutting through lava sheets (red outlined area) visible on a Sentinel 2-scene.

In order to reveal spatial relationships between dykes, the Euclidean distance and dyke density was calculated in ArcGIS. The Euclidean distance was derived from the digitized dykes. The output raster contains the measured distance from

every cell to the nearest source, in this case dykes. The distance of the dykes visualized in **Figure 8** provides an overview where the dykes occur concentrated and with less distance to each other.

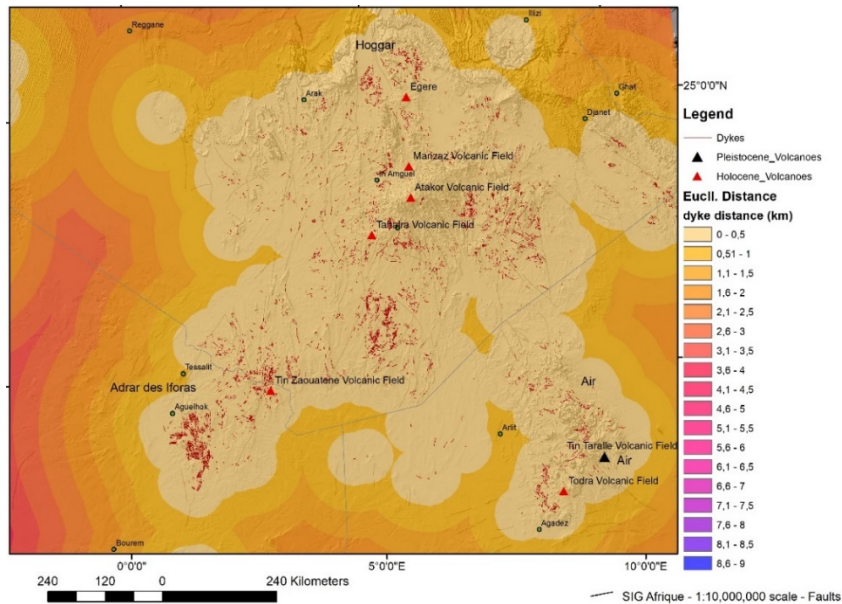
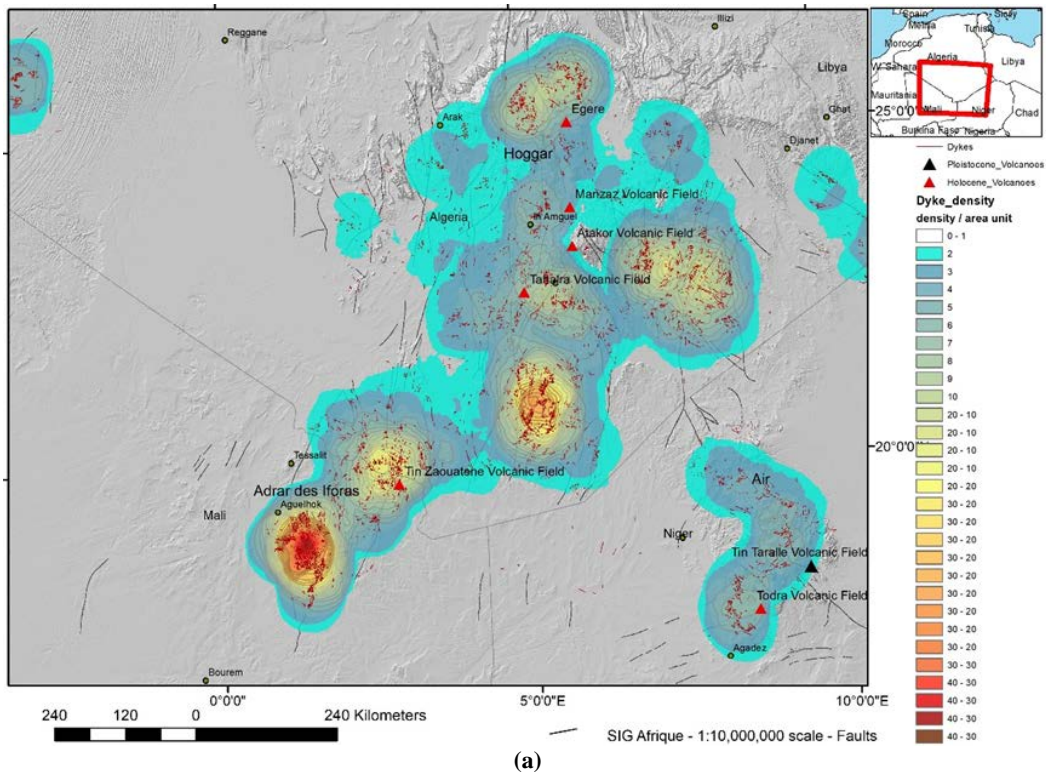


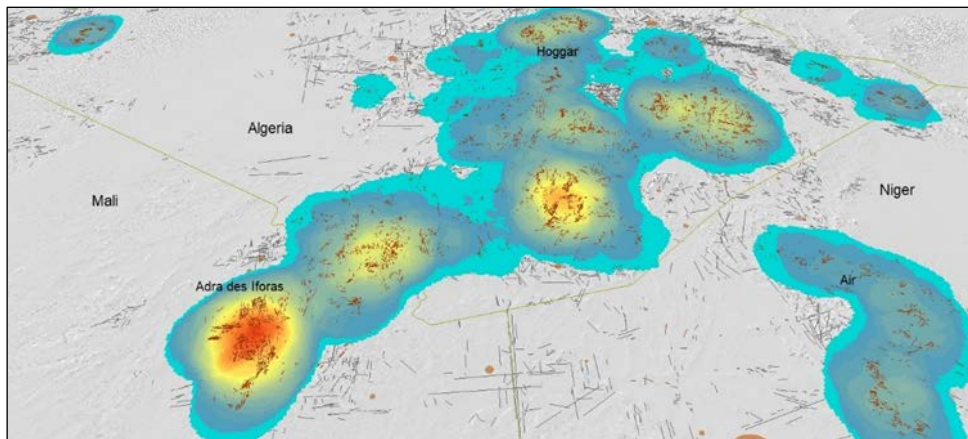
Figure 8. Euclidean distance of dykes.

This is achieved as well by a density calculation in ArcGIS: the density of the digitized dykes per unit area was calculated (**Figure 9a and b**) and,

then, the areas with a relatively higher dyke occurrence were investigated more detailed.



(a)



(b)

Figure 9. (a) Density of dyke occurrence; (b) 3D perspective view looking towards north.

The highest density of dykes striking predominantly NNW-SSE was detected in the Adrar des Iforas area in N-Mali within the Kidal-terrane, mainly comprising basement gneisses and calc-alkaline granitic plutons^[26]. The Adrar des Iforas is situated within the Pan-African mobile belt bordering the West-African craton in north-eastern Mali. It is characterized by major N-S shear zones parallel to the border of the craton which delimit longitudinal blocks, some of which have undergone horizontal displacements. Magmatic and tectonic Permo-Jurassic activity has been triggered by intraplate stress focused along the pre-existing Pan-

African suture zone^[27]. The Adrar des Iforas mountains have been affected by the Pan-African orogenesis (about 550–50 million years ago). This time period was characterized by injections of several generations of dykes, varying in their mineralogic composition such as basic, dioritic and dacitic dykes^[27]. The central part of the Iforas consists mainly of reactivated Pre-Pan-African basement that was intruded by Pan-African syn- and post-tectonic intermediate and acid plutonic rocks^[28]. The Cambrian strata are superimposed on the Pan-African by composite calc-alkaline batholiths in the Western Iforas, including the mainly N-S-oriented acid dyke swarms^[28].

The relatively higher dike density might be explained by uprising magma, that (by updoming the strata above) intensified fracturing processes and by the reactivation of existing fault zones. Dykes intruded into these zones of weakness. The high density of dykes in the Adrar des Iforas mountains might be influenced by the large batholiths (forming ring structures and domes) and their impact on the stress pattern. The influence of the batholiths on the dike pattern is obvious as within the

large domes very few dykes could be detected, however, a lot in between and around the circular structures. A higher density of dykes could be used as an indicator for a relatively stronger tectonic strain. Most of the parallel dike swarms trace the N-S- and WNE-ESE-striking shear zones. The N-S striking shear zones are clearly visible on satellite images and presented as lineaments (black lines) in **Figure 10**.

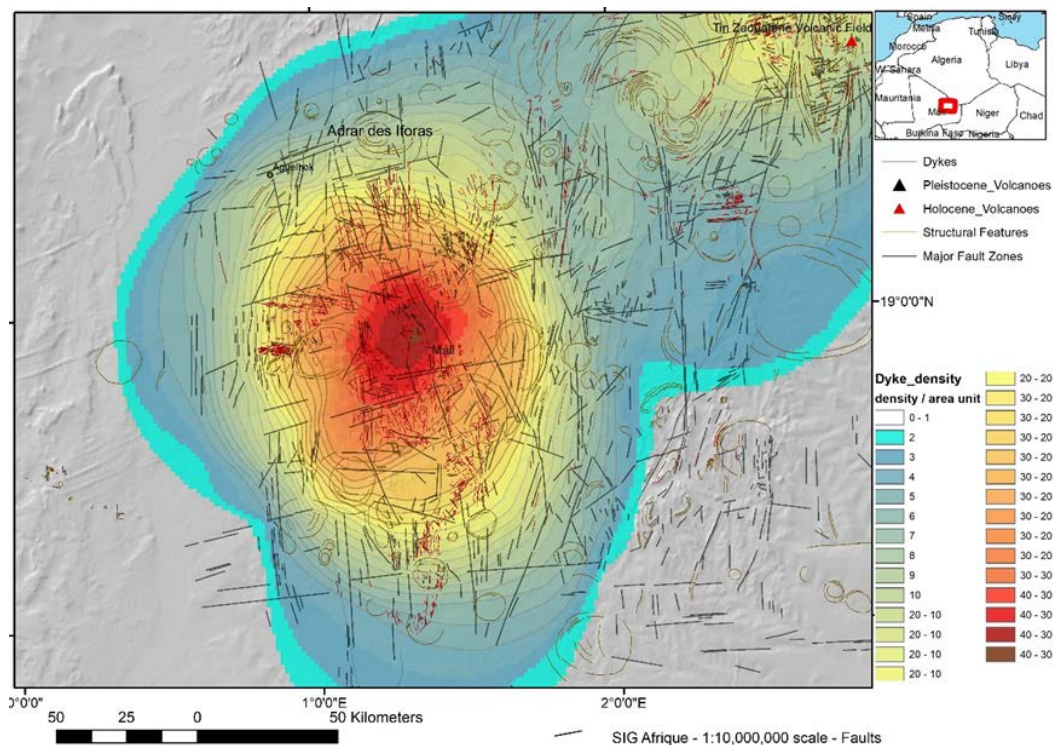


Figure 10. High dike density in the Adrar des Iforas mountains, N-Mali.

ALOS PALSAR radar images from the area with the highest density in **Figure 10** reveal dykes very clearly as white lines oriented in NNW-SSE and NNE-SSW direction as the ridges formed by the dykes in dense swarms cause a stronger radar reflection. Many dykes appear as irregular, interrupted lines (**Figure 11**).

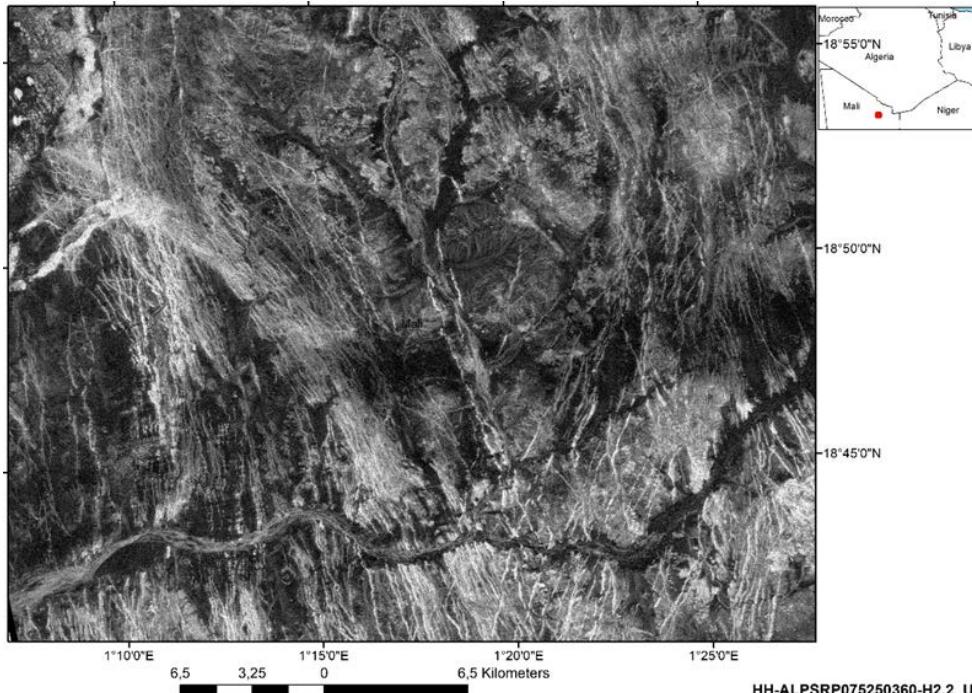
Figure 12a presents the same area indicating the main orientation of the dykes in a rose diagram and the length analysis of the visible dykes (**Figure 12b**). The majority of the dykes are extended over a length of about 200–400 m.

Dyke swarms can be detected as well in the northwest of the Adrar des Iforas mountains (**Figure 13**) building parallel, WNW-ESE-oriented

lines on the Landsat scene.

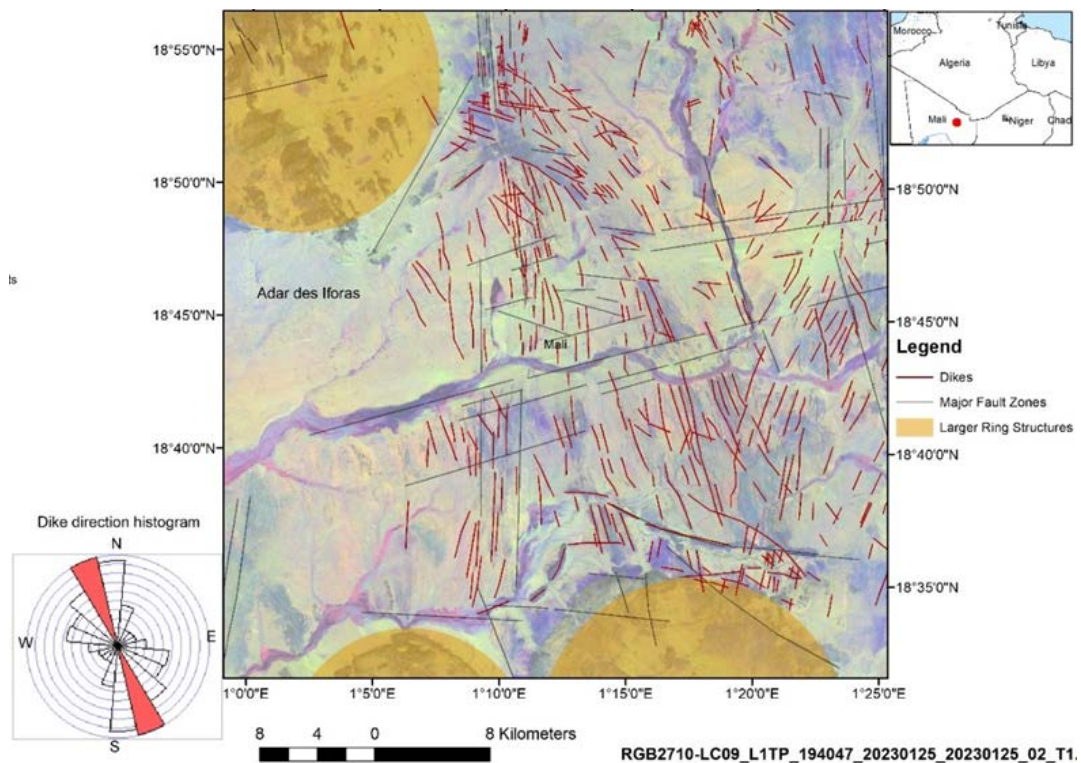
The next area with a relatively high dike occurrence and density is situated near the southern border of Algeria (**Figure 14**). Intrusion of dykes occurred here as well concentrated along the major shear zones in N-S and SW-NE directions.

The dykes in the southeastern part of the Hoggar mountains are often longer than those in N-Mali. Slope gradient maps derived from SRTM digital elevation model (DEM) data can be used for their identification (**Figure 15**) as demonstrated by the example situated in the SE of Algeria. The larger dykes with lengths of more than 10 km are clearly expressed on slope gradient maps.



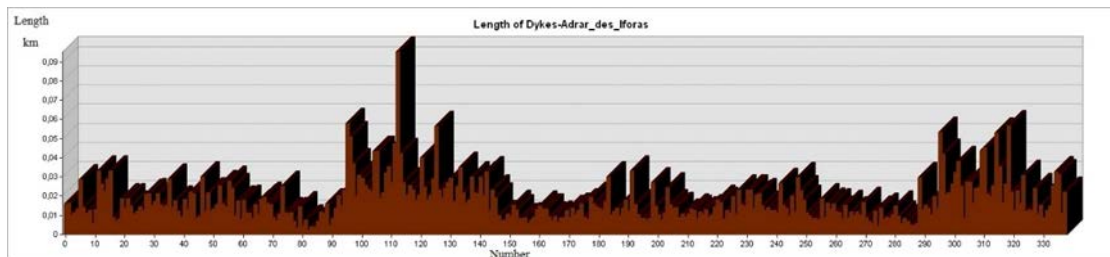
HH-ALPSRP075250360-H2.2-UA.

Figure 11. ALOS PALSAR radar scene of the northern part of the Adrar des Iforas mountains showing dykes as white lines cross cutting each other.



RGB2710-LC09_L1TP_194047_20230125_20230125_02_T1.

(a)



(b)

Figure 12. Orientation and length of the visible dykes in this area.

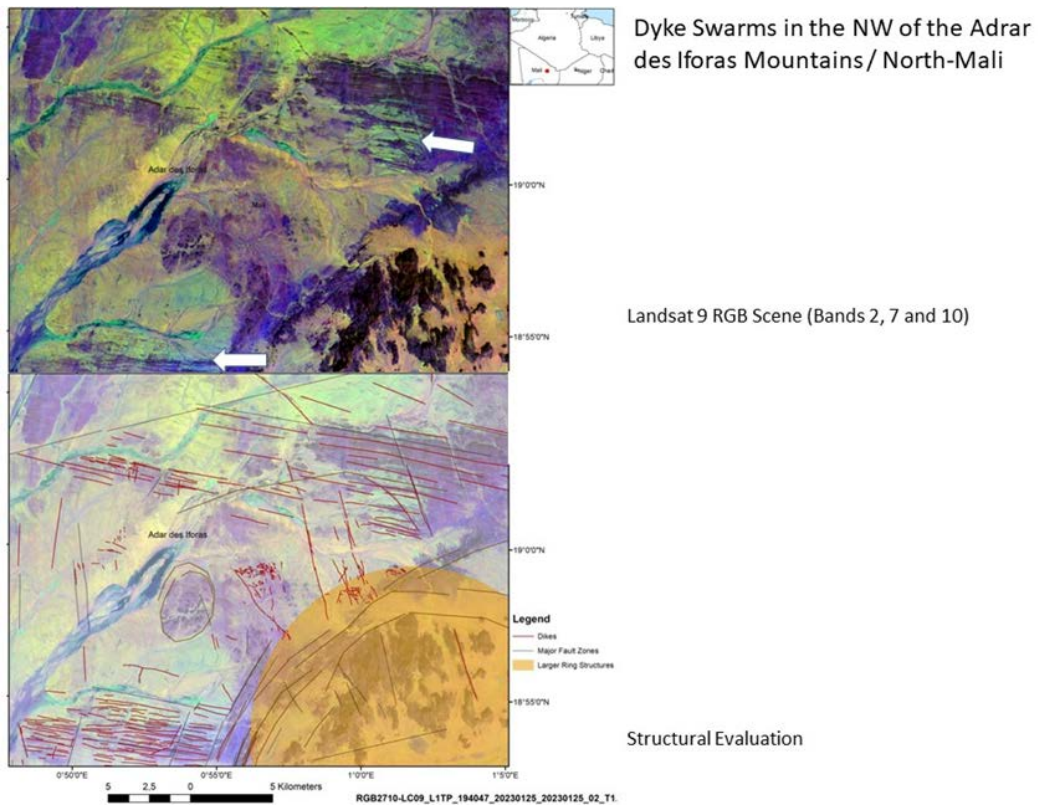


Figure 13. Dyke swarms in the NW part of the Adrar des Iforas mountains.

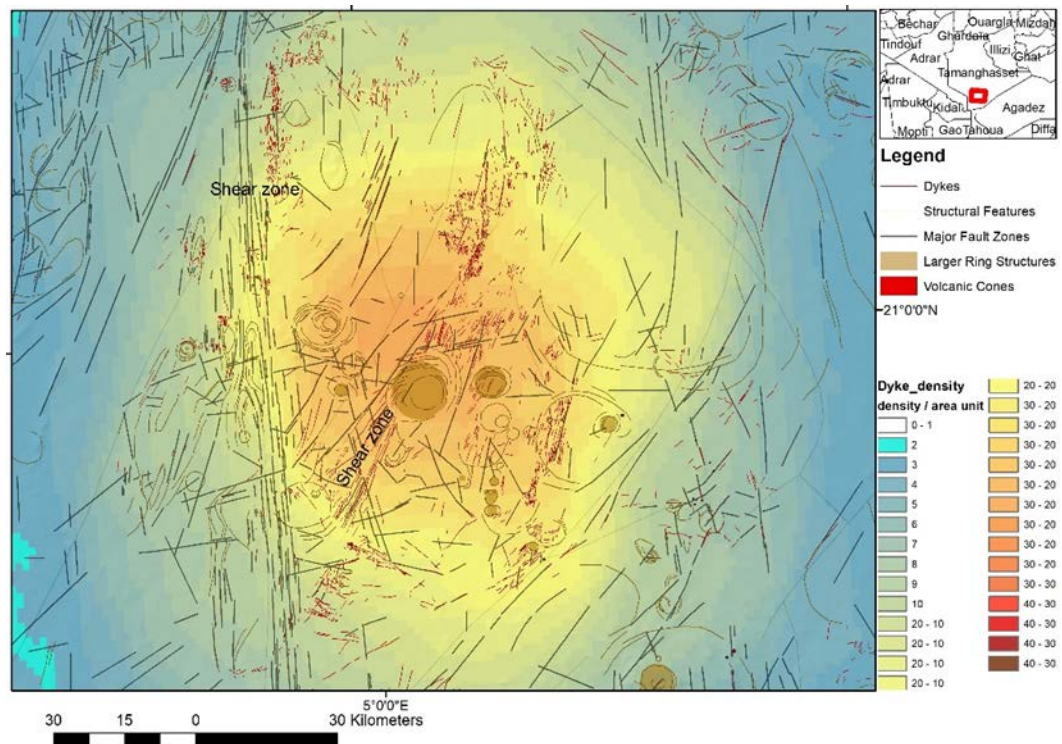


Figure 14. Dyke density influenced by shear zones in S-Algeria.

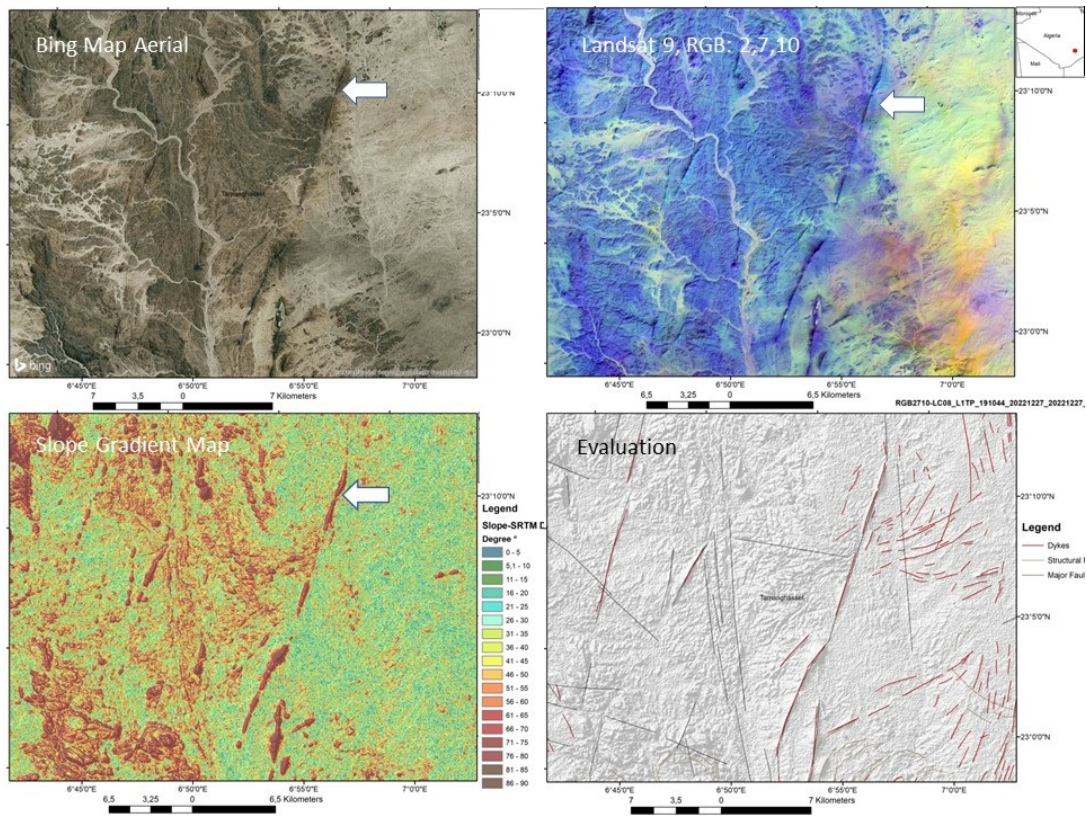


Figure 15. Combined analysis of different data sets for the inventory of dykes.

Besides the dykes, scoria cones and maars were digitized in the study area as well. To analyze whether there is a relationship between the appearance of volcanic features and the those of dykes, the density of the occurrence of volcanic cones and the density of dykes was compared. In the central and northern part of the Hoggar mountains, a spatial correlation between dyke occurrence and volcanic activity can be stated, as well as in the Air mountains. A higher density of dykes corresponds to the higher density of scoria cones related to Cenozoic magmatic activity. The Cenozoic volcanism was accompanied by uplift^[18] and, thus, enabling the development and reactivation of fracture and fault zones used by dyke intrusions. However, in the southern Hoggar and in the Adrar des Ifores mountains, such a spatial correlation is not visible (Figure 16). In these areas, tectonic strain seems to be the main reason for the high dyke concentration.

When dealing with the investigations of these relationships, the question about the age sequences arises: more detailed local information of the time periods of the dyke development, sequences and circumstances and the time periods of recurrent ac-

tivities of volcanism are needed for a better understanding of the complex interactions.

With regard to the cosmic impact craters, it can be observed that within the areas surrounding the impact craters in Central-Algeria, no dykes could be detected (Figure 17). As the magma chambers underneath the Hoggar mountains are estimated to exist in depths of about 150 km, the probability of initiating magmatic activity by a larger cosmic impact is relatively higher than in the environment. One possible explanation for this might be that the crust would have rebounded upward after the cosmic impact, temporarily decompressing the mostly solid mantle and causing it to melt and trigger uprising of magma. This could have been the case as shown in Figure 18. In N-Niger, ring dykes are visible along an assumed impact structure.

5. Conclusions

Remote sensing and GIS methods are useful tools for the systematic and standardized inventory of dykes that are visible at the surface, as well as for their structural environment. The comparative and combined evaluations of different satellite data

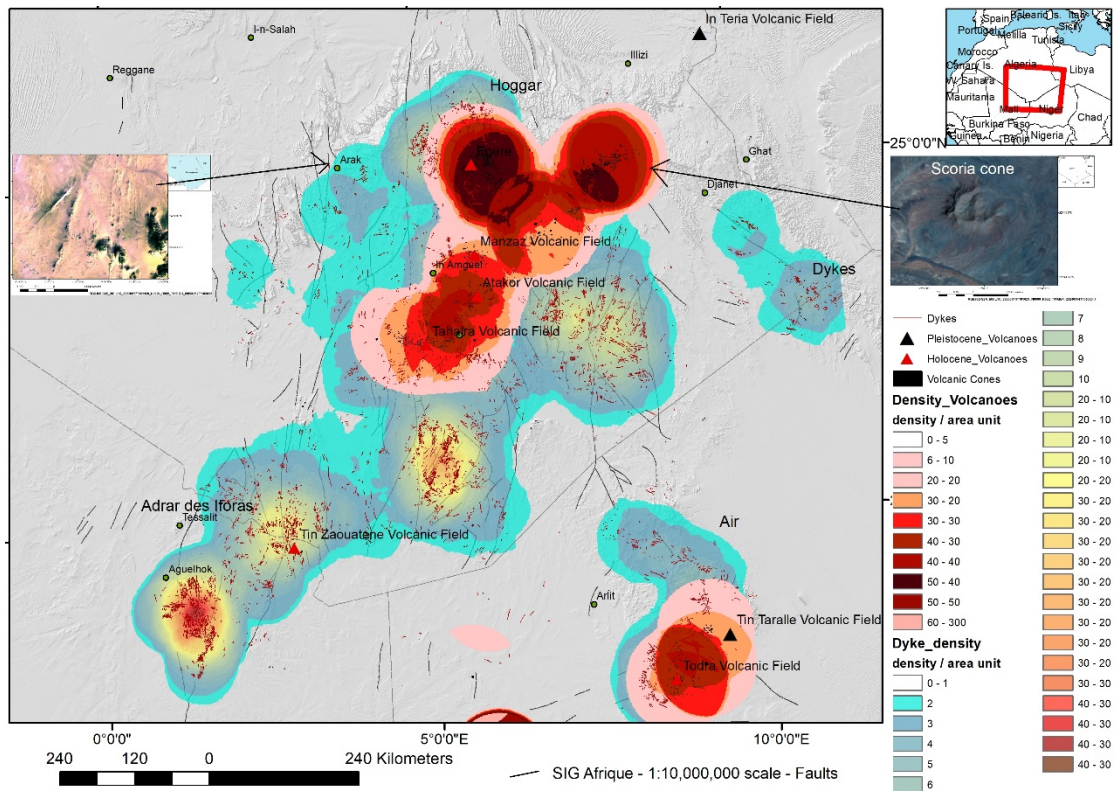


Figure 16. Overlay of the density calculation of dykes and of volcanic cones.

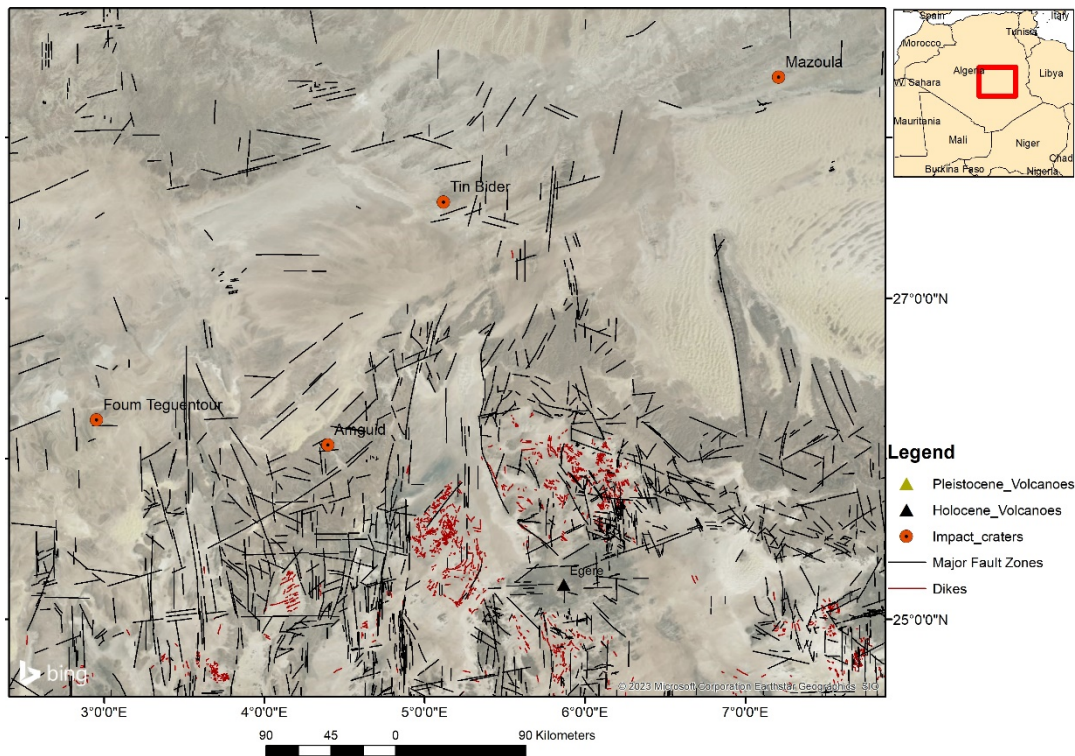


Figure 17. Impact craters in Central-Algeria without visible influence on dyke occurrence.

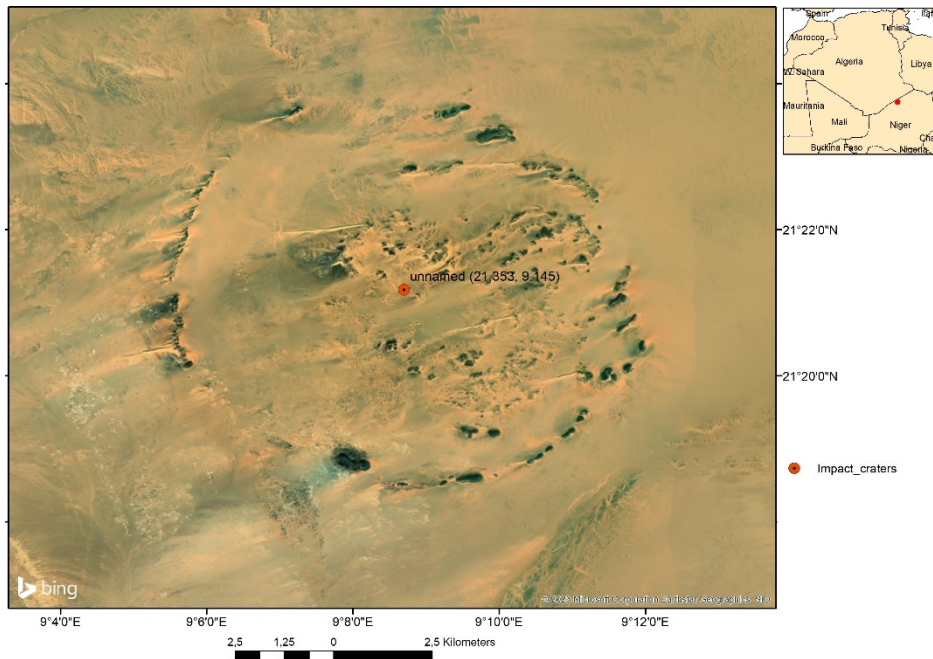


Figure 18. Ring dykes surrounding an assumed impact crater as documented in the impact crater data base from the Planetary and Space Science Centre (PASSC)^[11], Canada visible on a Bing Map scene.

embedded in a GIS support the mapping and morphologic analysis of dykes.

The occurrence of dykes seems to be related to a relatively higher strain and to magmatic activity. The following main factors appear to have an influence on the distribution and occurrence of dykes:

- transcurrent, horizontal movements along ductile north-south mega-shear zones, especially reactivated due to the Europe-Africa collision^[30],
- vertical movements (uplift),
- high-level plutons aligned on the mega-shear zones influencing the distribution pattern of dykes,
- properties of the host-rocks and higher strain conditions.

One of the main scientific tasks is to assess the likelihood of dykes reaching the surface to erupt^[6]. Prerequisite for this task is the knowledge about the occurrence of dykes, their ages and mineralogic composition as well as their structural setting. The hereby presented, standardized approach of the inventory of dykes is one of the steps in this direction. Using the same data sets such as Landsat RGB images combining the Bands 2, 7 and 10, Sentinel 2 RGB images, ALOS PALSAR L-Band images (15 m) and Sentinel 1 radar data over the large investigation area allows the mapping of dykes under

nearly the same conditions. Of course, when digitizing dykes based on the different satellite data without field work, the results cannot be complete and without errors. Sedimentary covers, especially dune fields, lack of tonal and morphological differences or small sizes (below the spatial resolution of the satellite data) are some of the reasons. Nevertheless, the evaluation results can support the planning of the necessary field work.

Density calculations of the digitized dykes contribute to the acquisition of areas with relatively higher concentration of dykes and, thus, indirectly to the detection of those areas with some of the above outlined properties. As geophysical and geodetic data of the Sahara region that would provide additional information are still scarce^[31] or not public available, the evaluation of satellite data provides a data base that can contribute to the support of further investigations.

Funding

This research received no external funding.

Acknowledgments

The author thanks the team of EnPress Publisher/*Journal of Geography and Cartography* and the reviewers for the opportunity to publish in this journal and for all their input and efforts.

Conflict of interest

The author declares that she has no conflict of interest.

References

1. Mekkaoui A, Remaci-Benaouda N, Graine-Tazerout K. Mafic dikes at Kahel Tabelbala (Daoura, Ougarta Range, south-western Algeria): New insights into the petrology, geochemistry and mantle source characteristics. *Comptes Rendus Geoscience* 2017; 349(5): 202–211. doi: 10.1016/j.crte.2017.06.003.
2. Berraki F, Bendaoud A, Brahimi B, *et al.* Cartography and petrographic and mineralogical study of the dolerite dykes of L'In Ouzzal (Hoggar Occidental, Algeria) (French). *Photo-Interprétation European Journal of Applied Remote Sensing* 2012; (1–2): 26–34.
3. Theilen-Willige B. Detection of ring structures and their surrounding tectonic pattern in South-Algeria, North-Mali and North- Niger based on satellite data. *Energy and Earth Science* 2023; 6(2): 1–29. doi: 10.22158/ees.v6n2p1.
4. Babikera M, Gudmundsson A. The effects of dykes and faults on groundwater flow in an arid land: The Red Sea Hills, Sudan. *Journal of Hydrology* 2004; 297: 256–273. doi: 10.1016/j.jhydrol.2004.04.018.
5. Hou G. Mechanism for three types of mafic dyke swarms. *Geoscience Frontiers* 2011; 3(2): 217–223. doi: 10.1016/j.gsf.2011.10.003.
6. Bazargan M, Gudmundsson A. Dike-induced stresses and displacements in layered volcanic zones. *Journal of Volcanology and Geothermal Research* 2019; 384: 189–205. doi: 10.1016/j.jvolgeores.2019.07.010.
7. Maerten F, Maerten L, Plateaux R, Cornard PH. Joint inversion of tectonic stress and magma pressures using dyke trajectories. *Geological Magazine* 2022; 159 (11–12): 2379–2394. doi: 10.1017/S001675682200067X.
8. Heidbach O, Rajabi M, Reiter K, *et al.* World stress map database release 2016. V. 1.1. GFZ Data Services; 2016. doi: 10.5880/WSM.2016.001.
9. Burchard HG. Meteorite impact origin of yellowstone hotspot. *Open Journal of Philosophy* 2016; 6(4): 412–419. doi: 10.4236/ojpp.2016.64038.
10. Azzouni-Sekkal A, Liégeois JP, Bechiri-Benmerzoug F, *et al.* The “Taourirt” magmatic province, a marker of the closing stage of the Pan-African orogeny in the Tuareg Shield: Review of available data and Sr-Nd isotope evidence. *Journal of African Earth Sciences* 2003; 37: 331–350. doi: 10.1016/j.jafrearsci.2003.07.001.
11. Earth Impact Database: Africa. PASSC. Available from: http://passc.net/EarthImpactDatabase/New%20website_05-2018/Index.html.
12. General Bathymetric Chart of the Oceans, GEBCO. Available from: <https://www.gebco.net/>.
13. English KL, Redfern J, Bertotti G, *et al.* Intraplate uplift: New constraints on the Hoggar dome from the Illizi basin (Algeria). *Basin Research* 2016; 29(3): 377–393. doi: 10.1111/bre.12182.
14. Ouzegane K, Liégeois JP, Doukkari S, *et al.* The Egéré Paleo-Mesoproterozoic rifted passive margin of the LATEA metacraton (Central Hoggar, Tuareg Shield, Algeria) subducted and exhumed during the Pan-African orogeny: U-Pb zircon ages, P-T-t paths, geo-chemistry and Sr-Nd isotopes. *Earth-Science Reviews* 2023; 236: 104262. doi: 10.1016/j.earscirev.2022.104262.
15. Kourim F, Bodinier JL, Alard O, *et al.* Nature and evolution of the lithospheric mantle beneath the Hoggar swell (Algeria): A record from mantle xenoliths. *Journal of Petrology* 2014; 55: 2249–2280. doi: 10.1093/petrology/egu056.
16. OneGeology Portal. British geological survey. Available from: <http://portal.onegeology.org/OnegeologyGlobal/>.
17. Dostal J, Caby R, Dupuy C. Metamorphosed alkaline intrusions and dyke complexes within the Pan-African Belt of western Hoggar (Algeria): Geology and geochemistry. *Precambrian Research* 1979; 10(1–2): 1–20. doi: 10.1016/0301-9268(79)90016-0.
18. Liégeois JP, Benhallou A, Azzouni-Sekkal A, *et al.* The Hoggar swell and volcanism: Reactivation of the Precambrian Tuareg shield during Alpine convergence and West African Cenozoic volcanism. *Plates, Plumes, and Paradigms*. 2005; 388: 379–400.
19. Liégeois JP, Latouche L, Boughrara M, *et al.* The LATEA metacraton (Central Hoggar, Tuareg shield, Algeria): Behaviour of an old passive margin during the Pan-African orogeny. *Journal of African Earth Sciences* 2003; 37: 161–190. doi: 10.1016/j.jafrearsci.2003.05.004.
20. Liégeois JP. The Hoggar swell and volcanism, Tuareg shield, Central Sahara: Intraplate reactivation of Precambrian structures as a result of Alpine convergence. *MantlePlumes.org*. Available from: <http://www.mantleplumes.org/Hoggar.html>.
21. Yahiaoui R, Dautria JM, Alard O, *et al.* A volcanic district between the Hoggar uplift and the Tenere Rifts: Volcanology, geochemistry and age of the In-Ezzane lavas (Algerian Sahara). *Journal of African Earth Sciences* 2014; 92: 14–20. doi: 10.1016/j.jafrearsci.2013.12.001.
22. Bouzid A, Bayou B, Liégeois JP, *et al.* Lithospheric structure of the Atakor metacratonic volcanic swell (Hoggar, Tuareg Shield, southern Algeria): Electrical constraints from magnetotelluric data. In: Foulger GR, Lustrino M, King SD (editors). *The interdisciplinary earth: A volume in honor of Don L. Anderson*. Geological Society of America; 2015. p. 239–255.
23. USGS Earth Explorer. Available from: <https://earthexplorer.usgs.gov/>.
24. European Space Agency (ESA). Copernicus Open Access Hub. Available from: <https://scihub.copernicus.eu/dhus/#/home>.

25. Alaska Satellite Facility (ASF). Data Search Vertex. NASA Earth Data. Available from: <https://search.asf.alaska.edu/#/>.
26. Bosch D, Bruguier O, Caby R, *et al.* Orogenic development of the Adrar des Iforas (Tuareg Shield, NE Mali): New geochemical and geochronological data and geodynamic implications. *Journal of Geodynamics* 2016; 96: 104–130. doi: 10.1016/j.jog.2015.09.002.
27. Liégeois JP, Sauvage JF, Black R The Permo-Jurassic alkaline province of Tadhak, Mali: Geology, geochronology and tectonic significance. *Lithos* 1991; 27: 95–105. doi: 10.1016/0024-4937(91)90022-D.
28. Black R, Bamako H, Ball E, *et al.* Outline of the Pan-African Geology of Adrar des Iforas (Republic of Mali). *Geologische Rundschau* 1979; 68(2): 543–564. doi: 10.1007/BF01820806.
29. Liégeois JP, Black R. Alkaline magmatism subsequent to collision in the Pan-African belt of the Adrar des Iforas (Mali). *Geological Society Special Publication* 1987; 30: 381–401. doi: 10.1144/GSL.SP.1987.030.01.18.
30. Hadj-Kaddour Z, Liégeois JP, Demaiffe D, Caby R. The alkaline–peralkaline granitic post-collisional Tin Zebane dyke swarm (Pan-African Tuareg shield, Algeria): Prevalent mantle signature and late altpaitic differentiation. *Lithos* 1998; 45: 223–243. doi: 10.1016/S0024-4937(98)00033-4.
31. Boukhalfa Z, Bouzid A, Xu Y, *et al.* Magnetoteluric investigation of the Precambrian crust and intraplate Cenozoic volcanism in the Gour Oumelalen area, Central Hoggar, South Algeria. *Geophysical Journal International* 2020; 223(3): 1973–1986. doi: 10.1093/gji/ggaa432.